Global Ecology & Biogeography (2001) **10**, 621–637

ETEMA SPECIAL ISSUE

Representation of vegetation dynamics in the modelling of terrestrial ecosystems: comparing two contrasting approaches within European climate space

BENJAMIN SMITH[1,2], I. COLIN PRENTICE[1,2] and MARTIN T. SYKES[1] [1]*Climate Impacts Group, Department of Ecology, Plant Ecology, Ecology Building, University of Lund, S-22362 Lund, Sweden, and* [2]*Max-Planck Institute for Biogeochemistry, Postfach 100164, D-07701 Jena, Germany*

ABSTRACT

1 Advances in dynamic ecosystem modelling have made a number of different approaches to vegetation dynamics possible. Here we compare two models representing contrasting degrees of abstraction of the processes governing dynamics in real vegetation.

2 Model (a) (GUESS) simulates explicitly growth and competition among individual plants. Differences in crown structure (height, depth, area and LAI) influence relative light uptake by neighbours. Assimilated carbon is allocated individually by each plant to its leaf, fine root and sapwood tissues. Carbon allocation and turnover of sapwood to heartwood in turn govern height and diameter growth.

3 Model (b) (LPJ) incorporates a 'dynamic global vegetation model' (DGVM) architecture, simulating growth of populations of plant functional types (PFTs) over a grid cell, integrating individual-level processes over the proportional area (foliar projective cover, FPC) occupied by each PFT. Individual plants are not simulated, but are replaced by explicit parameterizations of their growth and interactions.

4 The models are identical in their representation of core physiological and biogeochemical processes. Both also use the same set of PFTs, corresponding to the major woody plant groups in Europe, plus a grass type.

5 When applied at a range of locations, broadly spanning climatic variation within Europe, both models successfully predicted PFT composition and succession within modern natural vegetation. However, the individual-based model performed better in areas where deciduous and evergreen types coincide, and in areas subject to pronounced seasonal water deficits, which would tend to favour grasses over drought-intolerant trees.

6 Differences in model performance could be traced to their treatment of individual-level processes, in particular light competition and stress-induced mortality.

7 Our results suggest that an explicit individual-based approach to vegetation dynamics may be an advantage in modelling of ecosystem structure and function at the resolution required for regional- to continental-scale studies.

Key words Competition, DGVM, ecosystem model, Europe, gap model, mortality, plant functional type, succession.

INTRODUCTION

Vegetation dynamics, in a modelling context, comprise the processes of competition for resources among individuals or plant functional types (PFTs) and their feedbacks on plant carbon assimilation and allocation, reproduction and survival. Recent developments in dynamic ecosystem modelling include a number of different representations of vegetation dynamics, varying in their generality from the spatially explicit, individual plant representation of models such as SORTIE (Pacala *et al.*,

Corresponding author: E-mail: ben@planteco.lu.se

1993, 1996), the MUSE modelling framework (Gignoux *et al.*, 1998), and TREEGRASS (Simioni *et al.*, 2000; see also Sharpe *et al.*, 1986; Czárán & Bartha, 1989; Menaut *et al.*, 1990; Busing, 1991), to the area-averaged, horizontally undifferentiated representation of the IBIS dynamic global vegetation model (Foley *et al.*, 1996; Kucharik *et al.*, 2000).

Highly generalized approaches using broadly defined plant functional types (PFTs) have been shown to capture successfully vegetation distributions, biomass and primary production at the resolution required for continental to global-scale studies (Cramer *et al.*, 2001; Kucharik *et al.*, 2000). A high degree of averaging of processes and structure is inherent in such models. This reduces the number of parameters needed to drive the models, improves computational speed and leads to more tractable predictions. However, the averaging is based on assumptions of homogeneity (e.g. in vertical and horizontal canopy structure) that break down at finer geographical scales, or when the objects to be modelled are more narrowly defined plant functional types (PFTs) or individual species.

Spatially explicit individual-based models have been used, for example, to study community dynamics and biogeochemical cycling at the local (stand) scale in forests and savannas (e.g. Menaut *et al.*, 1990; Busing, 1991; Pacala & Deutschman, 1995; Pacala *et al.*, 1996; Simioni *et al.*, 2000). Such models generally require prescription of a relatively large number of parameters, based in part on measurements within the actual stands being simulated. Extrapolation of the predictions obtained to coarser scales would require development of scaling rules (Pacala & Deutschman, 1995), but these are generally unknown. The amount of detail incorporated into such models implies that they would be too computation-intensive to be applied on a spatially extensive basis, for example, across a grid spanning a region or continent.

Both highly generalized approaches and spatially explicit individual-based approaches are therefore unlikely to be suitable for modelling vegetation dynamics at scales intermediate between the local ($< \approx 10$ km) and continental-to-global, which we refer to here as the regional scale. In this paper, we compare two approaches to modelling vegetation dynamics, which would represent the minimum and maximum levels of simplification of natural dynamics desirable within a regional- to continental-scale modelling framework (Sykes *et al.*, 2001). Both models include at their core the same physiologically based representations of plant-level carbon and water fluxes, and allocation of assimilated carbon to the four compartments: leaves, fine roots, sapwood and heartwood. Both also employ the same set of five PFTs, corresponding to the major woody plant groups occurring naturally in Europe, plus a grass type. The differences between the models are in the biological units simulated — individuals in one, populations of PFTs over a grid cell in the other — and in the ways these units interact to simulate competition for light and soil resources. Because the models are substantially identical except in the formulation of vegetation dynamics, they are ideally suited to a comparative study: differences in the predictions they make given the same climatic driving conditions must be related to the representation of vegetation dynamics, and not some other feature, such as a different formulation of photosynthesis.

We apply both models at a number of localities, spanning the ranges of the biologically relevant climate parameters, winter cold, growing season warmth and growing season drought, within Europe under the modern climate, comparing their predictions of vegetation composition to the potential natural vegetation.

THE MODELS

General descriptions of the two models are given below. Additional details, including the key process equations, are given in the Appendix (see Supplementary Material p. 636).

Individual-based model

The structures of the two models are shown schematically in Fig. 1. Model (a), called the General Ecosystem Simulator (GUESS; B. Smith, I.C. Prentice, S. Sitch & M.T. Sykes, unpublished), simulates the growth of individuals on a number of replicate patches, corresponding in size approximately to the maximum area of influence of one large adult individual (usually a tree) on its neighbours. Patches are independent in terms of physical resources; that is, plants on different patches do not affect one another in the capture of light or uptake of water. However, patches are assumed to be close enough together to share a common propagule pool, establishment of new

saplings of each PFT after initial colonization being directly related to the reproductive output of all individuals of that PFT the previous year (the 'spatial mass effect'; Shmida & Ellner, 1984).

Each woody individual belongs to one PFT (cf. taxon), with its associated parameters controlling establishment, phenology, carbon allocation, allometry, survival response to low light conditions, scaling of photosynthesis and respiration rates and the limits of the climate space the PFT can occupy. Carbon taken up through photosynthesis, and remaining following deduction of respiration and reproduction costs, is partitioned among the compartments leaf mass, fine root mass and sapwood mass, subject to certain constraints (including a constant ratio of sapwood cross-sectional area to leaf area; the pipe model of Shinozaki *et al.*, 1964), and to the balance between light and water limitation to photosynthesis (Haxeltine & Prentice, 1996). Each simulation year, a PFT-specific proportion of leaf mass and root mass is turned over (lost to individuals), and a fixed proportion of sapwood is converted to heartwood: relatively more for shade-intolerant PFTs. Stem diameter, crown area and plant height are related to the sum of sapwood and heartwood mass (Huang *et al.*, 1992; Zeide, 1993), while bole height (the minimum height reached by the crown cylinder of each tree) is controlled by a PFT-specific minimum PAR level for photosynthesis.

Individuals are not distinguished for grasses. A layer of grass at ground level in each patch is treated as two 'individuals' — one each with the C3 and C4 photosynthetic pathways. Each grass is represented by patch totals of leaf and root carbon. Partitioning of assimilated carbon is done according to the balance between water and light limitation, as for trees.

Carbon uptake through photosynthesis, plant evapotranspiration and soil water content are calculated on daily (for water balance) and monthly (photosynthesis) timesteps by a coupled photosynthesis and water module derived from the BIOME3 equilibrium biosphere model (Haxeltine & Prentice, 1996). The amount of carbon fixed by each individual each year is influenced by the quantity of photosynthetically active radiation (PAR) captured and by stomatal conductance, the latter being reduced when atmospheric evapotranspirational demand exceeds the maximum transpiration rate with fully open stomata, i.e. in the presence of water stress.

The fraction of incoming PAR captured by each individual across its crown area is calculated daily using the Lambert–Beer law (Monsi & Saeki, 1953), which represents an exponential reduction in available light through the canopy, based on the accumulated leaf area index (LAI, the ratio of accumulated leaf area to ground area) above a given height in each patch (Prentice & Leemans, 1990). Sun angle is not directly taken into account. PAR reaching ground level, and exceeding a minimum level for assimilation, is taken up by grasses, which are assumed to cover the entire patch area (partitioned between the C3 and C4 types according to their relative LAIs). The amount of carbon available for allocation at the end of a simulation year is reduced by maintenance and growth respiration, leaf and root turnover, and a fixed fractional allocation to reproduction for mature woody plants and all grasses.

Model formulations of establishment and mortality are based on those employed within the 'forest gap' model FORSKA (Leemans & Prentice, 1989; Prentice *et al.*, 1993). The number of new saplings of each woody PFT and in each patch each year is drawn at random from the Poisson distribution, with an expectation influenced by a PFT-specific maximum establishment rate and by the 'propagule pool', i.e. the amount of carbon allocated to reproduction by all individuals of the PFT at all patches the previous year. No saplings are established in a given patch if the minimum PAR level at the forest floor is below a PFT-specific threshold, which is higher for more light-demanding species.

Mortality of individuals is stochastic and is based on the sum of a background rate, inversely related to the PFT-specific mean non-stressed longevity, and a much higher rate, imposed only when the 5-year average mean growth efficiency (the ratio of individual net annual production to leaf area) falls below a PFT-specific threshold. The latter is higher for more light-demanding species.

Area-based model

In contrast to the individual-based model, in which differences in size and form among individuals influence their resource capture and subsequent growth, model (b) (Fig. 1), an adapted version of the LPJ (Lund-Potsdam-Jena) dynamic global vegetation model (Sitch, 2000; S. Sitch, I.C. Prentice,

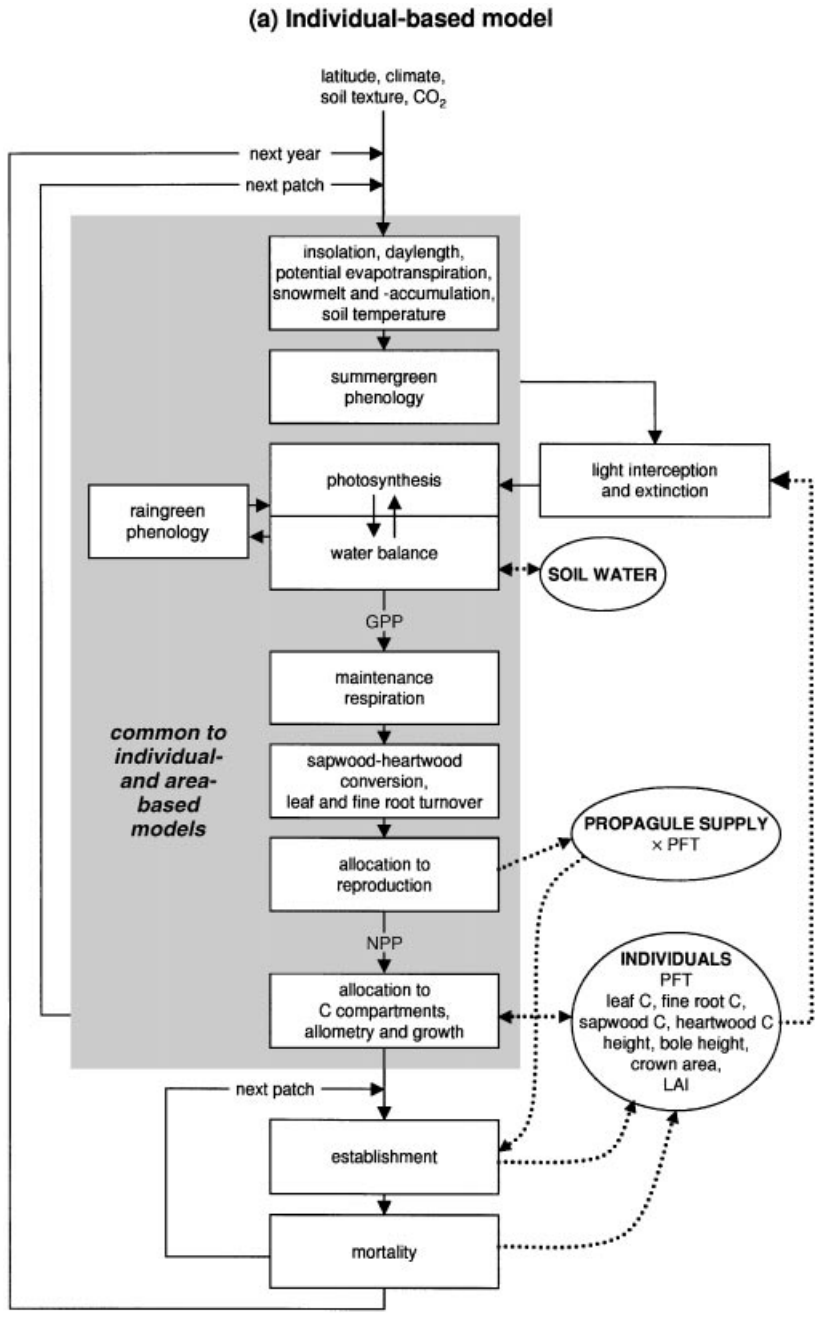

Fig. 1 Two ecosystem models differing in the representation of vegetation structure and dynamics: (a) a patch model in which individuals are distinguished and compete for light and soil water with other individuals in the same patch ('individual-based model'); (b) a model in which individual characteristics and patch differences are averaged across a larger area for each of a number of plant functional types (PFTs) ('area-based model'). Modules dealing with determination of environmental drivers, phenology, photosynthesis and water balance, respiration, leaf and root turnover, carbon allocation and tree allometry are common to both models.

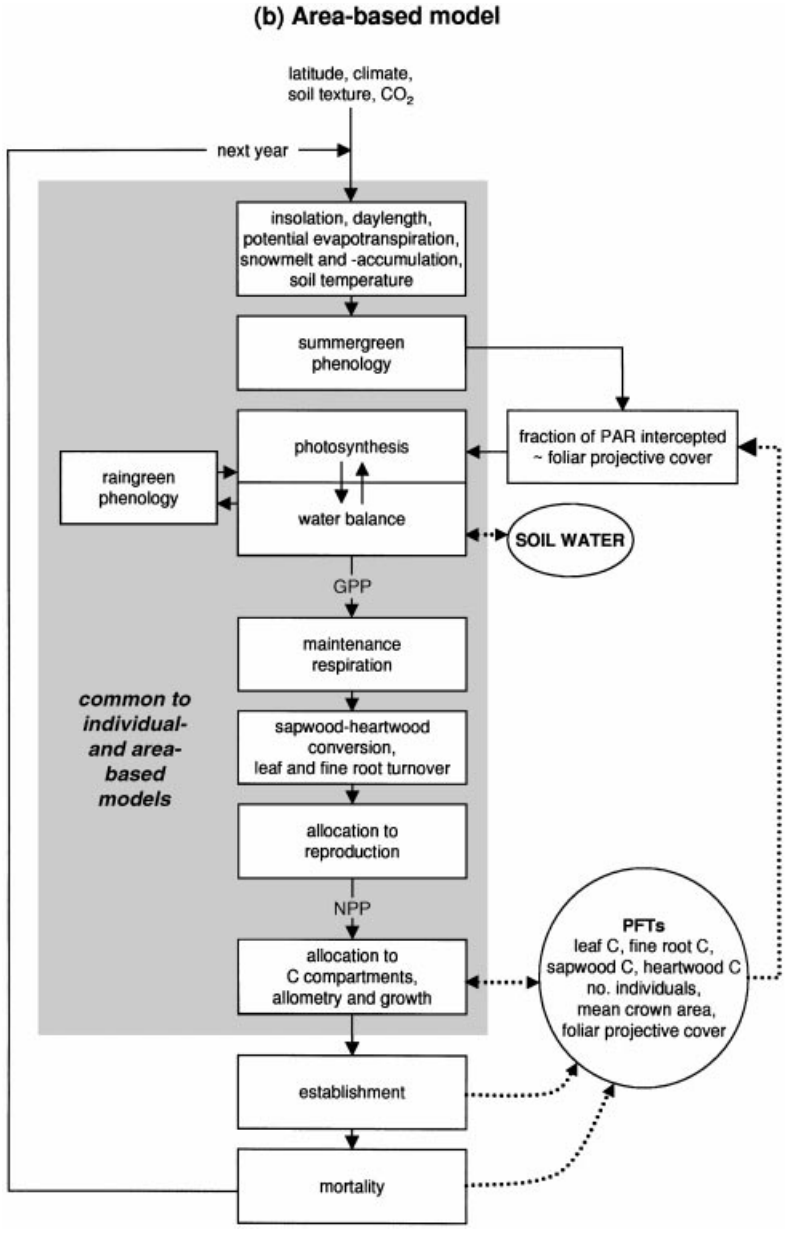

Fig. 1 *continued.*

B. Smith & LPJ Consortium Members, unpublished), implicitly averages individual and patch differences across a wider area and across 'populations' of PFTs. The approach has the advantage of being far less computation-intensive and, since intrinsically stochastic parameters such as establishment and mortality rates can be specified as averages, the predictions obtained are deterministic, and there is no need to perform multiple simulations, or to model a number of replicate patches,

as required with the individual-based model. The principal disadvantage of the area-averaging approach is that the processes of competition for light and soil resources, which are essentially neighbourhood phenomena in nature, cannot be represented in a very mechanistic way. This might give rise to less robust predictions when the model is run using different environmental (climate/radiation/CO_2, etc.) drivers from those under which it was calibrated.

Woody PFTs are represented by the density of individuals per unit area and carbon content per unit area in the four compartments leaf mass, fine root mass, sapwood mass and heartwood mass, as averages across the area modelled. Mean stem diameter, height and crown area are calculated from the sum of sapwood and heartwood mass per individual, using the same set of allometric relationships as in the individual-based model. Grasses are represented only by the leaf and root compartments.

Foliar projective cover (FPC), the proportion of ground area covered by leaves, is calculated for each PFT as the product of the fraction of incident PAR absorbed (from the Lambert–Beer law, given mean individual LAI), mean individual crown area and mean number of individuals per unit area. The sum of FPCs for all PFTs is constrained to remain ≤ 1, the difference representing ground area remaining to be colonized. PFTs 'compete' for occupation of space through growth, which can increase their FPC.

Carbon uptake is modelled, as in the individual-based model, using the BIOME3 coupled photosynthesis and water balance module, but the photosynthesis values obtained are area-based averages for each PFT (i.e. gross primary production, GPP), rather than totals for each individual as in the other model. The fraction of PAR captured is the FPC, multiplied by one-half to account for losses to non-photosynthetic structures and to the soil (Landsberg, 1986; Haxeltine & Prentice, 1996). Net primary production (NPP), the amount of carbon per unit area remaining for allocation to plant tissues, is reduced by maintenance and growth respiration, leaf and root turnover, and allocation to reproduction, which are modelled using the same formulations as in the individual-based model.

Establishment and mortality are modelled in as similar a way as possible to the individual-based model, given that each PFT is represented only by one 'average individual' and by the spatial density of individuals. Establishment takes place each simulation year. The number of new 'saplings' per unit area is proportional to a PFT-specific maximum establishment rate and to the current FPC of the PFT concerned (a spatial mass effect), and declines in proportion to canopy light attenuation when the sum of woody FPCs exceeds 0.9 and approaches 1, simulating a decline in establishment success with canopy closure (Prentice *et al.*, 1993). New saplings are allowed only in the proportion of the grid cell not covered by woody vegetation, and this proportion may be reduced further by the total fractional area in which the mean forest-floor PAR level is below a PFT-specific threshold (which is higher for more light-demanding PFTs). New saplings have the effect of increasing the number of individuals per unit area, and adjusting other PFT state variables to reflect the new population means. The net effect is always a marginal increase in FPC.

Mortality is modelled by a fractional reduction in all state variables, including the number of individuals per unit area. A background mortality rate, the inverse of mean PFT longevity, is applied each year. An additional stress mortality rate has two components, one inversely related to mean growth efficiency (which would be negatively influenced by, e.g. drought), the other to 'shading', which is assumed to increase exponentially as the sum of woody FPCs approaches 1. Light-demanding PFTs experience a higher rate of shading mortality than shade-tolerant ones. The net effect of mortality is a marginal decrease in FPC, creating new space for PFT expansion by growth and establishment.

THE EXPERIMENT

To perform a comprehensive test of the relative performance of the individual- and area-based models within the range of climates prevailing in Europe, we first developed a classification of the European continent into bioclimatic zones. We focused on three variables that are strongly associated with the distribution of different functional types of plants at the regional to global scale: winter temperatures (characterized by the mean temperature of the coldest month, T_c), growing season warmth (characterized by growing degree days, GDD_5, the annual sum of: max[0, T-5], where T is daily mean temperature in °C) and growing

Table 1 Bioclimatic zones for Europe based on climatic indices of: drought tolerance (α^*_{min}, minimum growing season ratio of actual transpiration to equilibrium evapotranspiration); temperature of coldest month (T_c); and growing degree days (GDD_5, on 5 °C base)

Bioclimatic zone	α^*_{min}	T_c (°C)	GDD_5
1	< 0.4	< –1.5	< 700
2	< 0.4	< –1.5	700–1500
3	< 0.4	< –1.5	1500–2500
4	< 0.4	–1.5–1.5	700–1500
5	< 0.4	–1.5–1.5	1500–2500
6	< 0.4	< 1.5	> 2500
7	< 0.4	> 1.5	1500–2500
8	< 0.4	> 1.5	> 2500
9	> 0.4	< 1.5	> 2500
10	> 0.4	> 1.5	> 2500

season drought (characterized by the Priestley–Taylor coefficient, α^*_{min}, the minimum ratio of actual transpiration to equilibrium evapotranspiration, for the period with temperatures ≥ 5 °C; Sykes *et al.*, 1996). We chose boundary values of these variables that correspond to observed limits of major taxa or functional types: $T_c = -1.5$, marking the southern and low-altitude limit of norway spruce, *Picea abies* (nomenclature follows Tutin *et al.* (1964–80)); $T_c = 1.5$, corresponding approximately to the cold limit of the temperate evergreen tree *Quercus ilex*; $GDD_5 = 700$, 1500, 2500, minimum summer warmth limits for various European broadleaved tree species; and $\alpha^*_{min} = 0.4$, the approximate minimum drought limit for Mediterranean shrubland vegetation (Sykes *et al.*, 1996; M.T. Sykes, unpublished). The resulting classification gives 10 bioclimatic zones of spatial significance for Europe (Table 1; Fig. 2). We chose one locality within each zone (two localities, one Arctic, the other Alpine, for zone 1) as test sites for the model comparison, favouring sites for which the natural vegetation is well documented.

The same set of five PFTs was used for both models and at all sites (Table 2). Where possible, parameters were assigned based on values or relationships reported in the literature (Fulton, 1991; Prentice & Helmisaari, 1991; Reich *et al.*, 1992; Haxeltine & Prentice, 1996; Sykes *et al.*, 1996). Full details of how these parameters influence the simulations are given in the Appendix (see Supplementary Material p. 636). The four woody PFTs correspond to the major functional groups of European trees, encompassing the following more important taxa, among others:

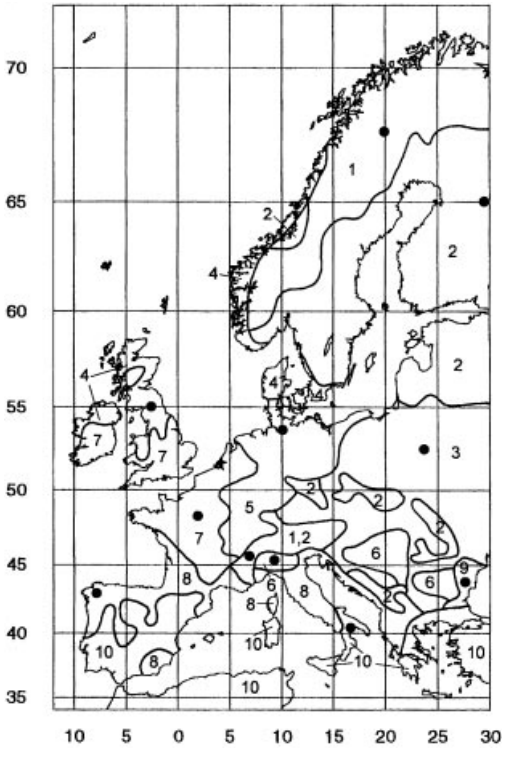

Fig. 2 Bioclimatic zones for Europe, as defined in Table 1, showing locations (dots) of test sites for model experiment.

Boreal/temperate needle-leaved evergreen (NE): *Picea abies*, *Pinus sylvestris*, *Abies alba*.

Temperate shade-tolerant broadleaved summergreen (TBS): *Fagus sylvatica*, *Carpinus betulus*, *Fraxinus excelsior*, *Tilia* spp., *Ulmus* spp., *Castanea sativa*, deciduous *Quercus* spp.

Boreal/temperate shade-intolerant broadleaved summergreen (IBS): *Betula* spp., *Salix* spp., *Populus* spp., *Sorbus aucuparia*.

Temperate broadleaved evergreen (BE): *Quercus ilex*, *Quercus suber*, *Ilex aquifolium*, *Laurus nobilis*.

Each model was run from 'bare ground' for a period of 2000 simulation years, the maximum needed to achieve an equilibrium solution. Environmental drivers (monthly air temperature,

Table 2 Parameters distinguishing the five plant functional types (PFTs) used in runs of both the individual- and area-based model. NE = boreal/temperate needle-leaved evergreen; TBS = temperate shade-tolerant broadleaved summergreen; IBS = boreal/temperate shade-intolerant broadleaved summergreen; BE = temperate broadleaved evergreen; G = grass; T_c = mean temperature of the coldest month; GDD_5 = growing degree days on 5 °C base; E = evergreen; S = summergreen; R = raingreen; SLA = specific leaf area. Mathematical symbols are referred to in the Appendix (see Supplementary Material, p. 636)

Parameter	Plant functional type					
	Symbol	NE	TBS	IBS	BE	G
Min. T_c for survival (°C)		—	–18.0	—	1.7	—
Min. GDD_5 for reproduction		—	1000	—	2500	—
Max. T_c for reproduction (°C)		–1.0	6.0	—	—	—
Chilling requirement for budburst		—	yes	—	—	—
Max. establishment rate (saplings/year)	est_{max}	10	10	20	15	—
Min. PAR flux for establishment (Wm^{-2})	par_{min}	4.05	4.05	9.25	4.05	—
Fulton (1991) recruitment shape parameter	α	1.0	0.3	3.0	0.3	—
Mean non-stressed longevity (years)	long	300	200	150	200	—
Growth efficiency threshold (gC m^{-2} $years^{-1}$)	$greff_{min}$	90	50	90	70	—
Leaf phenology		E	S	S	E	E, S or R
Fraction of roots in upper/lower soil layer		0.33/0.67	0.33/0.67	0.33/0.67	0.33/0.67	0.67/0.33
Max. leaf : root C mass ratio	ltor	1.0	1.0	1.0	1.0	0.5
Leaf turnover rate ($year^{-1}$)	$turn_{leaf}$	0.33	1.00	1.00	0.33	1.00
Fine root turnover rate ($year^{-1}$)	$turn_{root}$	0.5	1.0	1.0	0.5	0.5
Sapwood turnover rate ($year^{-1}$)	$turn_{sapwood}$	0.1	0.1	0.2	0.1	—
SLA (cm^2 $[gC]^{-1}$)	SLA	93	273	243	132	324
Min. canopy conductance (mm s^{-1})	g_{min}	0.3	0.5	0.5	0.5	0.5
Optimal temp. range for photosynthesis (°C)		10–25	15–25	10–25	15–35	10–45
Maintenance respiration coefficient	r	1.00	1.00	1.00	1.00	0.15

precipitation and fractional sunshine) were derived from the CLIMATE observational data base (W. Cramer *et al*. unpublished). An atmospheric CO_2 concentration of 340 p.p.m.v. was assumed. The same climatic and radiative conditions were assumed each simulation year. The individual-based model was run with 10 replicate patches, which is sufficient to achieve a relatively stable 'equilibrium' PFT composition.

RESULTS AND DISCUSSION

Both models were successful in predicting the PFT composition of the observed natural vegetation at the majority of test sites (Table 3). At many sites, the natural vegetation appears to correspond more closely to the model PFT composition after 250 simulation years, rather than the equilibrium composition, achieved after 2000 years of 'succession'. At year 250 the shade-intolerant PFT (ITS) is codominant or even dominant at several sites, whilst it becomes absent or almost so at equilibrium, being replaced by one of the more shade-tolerant woody types (e.g. Bialowieza, Derborence, Galicia; Figs 3, 4). Both models tend to generate a classical successional series in which herbaceous ruderal species (represented by the grass PFT) are replaced first by fast-growing but light-demanding pioneer trees (IBS), which in turn succumb to competition by more shade-tolerant trees (NE, TBS or BE). In nature, pioneer species tend to be maintained by periodic disturbances, whereas in the present model experiment, disturbances were disallowed. Interruptions of the natural succession through natural and (especially) human disturbances occur regularly in nearly all vegetation types in Europe. Few large areas have remained undisturbed for more than the last 250 years. A close correspondence, at many sites, of the observed vegetation with model predictions for year 250 may therefore be cautiously interpreted as support for the model predictions. Model predictions for year 2000 correspond to the potential natural vegetation that might be expected were vegetation allowed to develop to equilibrium biomass and cover, in the absence of human influences or natural disturbances.

The ancient Bialowieza forest in north-eastern Poland includes apparently stable stands dominated by both needleleaved (*Picea abies*, *Pinus sylvestris*) and broadleaved (*Quercus* spp., *Carpinus betulus*, *Tilia cordata*) trees (Falinski, 1986). The individual-based model successfully predicts a stable mixture of the needle-leaved and shade-tolerant broadleaved PFTs at this site, whilst the area-based model predicts dominance by broad-leaved trees, with a very minor needle-leaved component, at equilibrium (Fig. 3). The individual-based model predicts a succession in which broadleaved light-demanding trees (at this site these would be *Betula pendula*, *B. pubescens* and/or *Populus tremula*) dominate initially, subsequently being replaced (completely by *c.* year 1000) by a mixture of needle-leaved trees (75%) and shade-tolerant broadleaved trees (25%). This temporal pattern matches reasonably a chronosequence of PFT fractional cover derived from separate 100-year chronosequences in 10 community types within the Bialowieza forest (Falinski, 1986; Fig. 3), although the observations suggest that exclusion of the shade-intolerant species may occur within much less than a millenium.

The individual-based model predicts a forest steppe in eastern Bulgaria (Table 3; Fig. 5), where the grass PFT accounts for the majority of NPP and LAI at equilibrium, the remainder (and still the majority of biomass) comprising shade-tolerant summergreen trees. This corresponds well to the natural vegetation of the western Black Sea coast, which is described by Walter (1979) as a macro-mosaic of meadow steppe and deciduous forest stands, a product of a dry growing season combined with freezing winter temperatures. The area-based model, however, predicts a deciduous forest with no grass for the same site. This difference between the two models appears to be a result of the parameterization of competition between woody PFTs and grasses in the area-based model, in which woody PFTs almost always prevail in competition with grasses (by taking over some of their FPC), even if soil water, rather than light, is actually the limiting resource. In the area-based model, grasses are able to persist at equilibrium only if the woody PFTs are unable to match the annual decrease in their FPC through mortality by a (marginally higher) establishment rate, and this is likely only at very high levels of drought. In the individual-based model, which includes explicit vertical structure, grasses can persist under a canopy of trees until the PAR flux reaching the forest floor falls below a minimum threshold. Under conditions of drought, NPP remains relatively

Table 3 Net primary production (NPP, kgC m^{-2} $year^{-1}$), leaf area index (LAI) and biomass (kgC m^{-2}) for five PFTs, predicted by the individual- and area-based models after 250 years and 2000 years of succession, under modern climate conditions at 11 climatically distinct sites in Europe. A description of the natural vegetation in each region is given for comparison with the model results. PFTs whose bioclimatic limits for establishment and/or survival prohibit occupancy of a particular site are not shown

Site	Bioclimatic zone	Simulation time (years)	PFT* comp.	Individual-based model			Area-based model			Natural vegetation
				NPP	LAI	Biomass	NPP	LAI	Biomass	
NW Lapland, 20°E 67°30′N	1	250	NE	0.05	0.4	1.5	0.01	0.1	0.1	Evergreen needle-leaf forest dominated by *Pinus sylvestris* and deciduous woodland dominated by shade-intolerant broadleaved trees (*Betula* spp., *Salix* spp. *Sorbus aucuparia*) (Påhlsson, 1994; Council of Europe, 1987)
			IBS	0.03	0.2	1.7	0.46	3.3	5.2	
			G	0.14	4.7	0.1	0.01	0.0	0.0	
		2000	NE	0.22	1.4	26.6	0.51	3.5	16.9	
			IBS	0.00	0.0	0.0	0.00	0.0	0.0	
			G	0.0	0.3	0.0	0.00	0.0	0.0	
N Karelia, 30°E 65°N	2	250	NE	0.01	0.7	3.1	0.01	0.1	0.1	Evergreen needle-leaf forest dominated by *Pinus sylvestris* and deciduous woodland dominated by shade-intolerant broadleaved trees (*Betula* spp., *Salix* spp., *Sorbus aucuparia*) (Påhlsson, 1994; Council of Europe, 1987)
			IBS	0.01	0.3	3.5	0.55	3.8	6.5	
			G	0.08	2.5	0.1	0.01	0.0	0.0	
		2000	NE	0.28	1.7	41.6	0.52	3.5	16.7	
			IBS	0.00	0.0	0.0	0.00	0.0	0.0	
			G	0.00	0.0	0.0	0.01	0.0	0.0	
S. Scotland, 03°W 55°N	4	250	TBS	0.05	0.4	1.7	0.05	0.4	0.7	Deciduous *Quercus* spp.-dominated forest, with *Betula pubenscens*-dominated woodland at higher elevations and as a seral component. Other shade-tolerant and light demanding broadleaved trees including *Fraxinus excelsior*, *Prunus avium*, *Ulmus glabra*, *Tilia cordata* and *Corylus avellana* (Council of Europe, 1987)
			IBS	0.07	0.3	6.7	0.68	4.1	9.0	
			G	0.18	5.8	0.2	0.01	0.0	0.0	
		2000	TBS	0.24	1.8	20.9	0.69	4.4	27.5	
			IBS	0.00	0.0	0.0	0.00	0.00	0.0	
			G	0.03	1.0	0.0	0.01	0.0	0.0	
Schleswig-Holstein, 10°E 53°30′N		250	TBS	0.08	0.6	3.3	0.16	1.2	1.9	Deciduous forest dominated by *Quercus* spp., *Fagus sylvatica*, *Betula pendula*, *Sorbus aucuparia* (Council of Europe, 1987)
			IBS	0.09	0.3	10.3	0.56	3.2	7.1	
			G	0.22	7.1	0.2	0.01	0.0	0.0	
		2000	TBS	0.35	2.5	32.6	0.74	4.5	28.6	
			IBS	0.00	0.0	0.0	0.00	0.0	0.0	
			G	0.03	1.0	0.0	0.01	0.0	0.0	

Table 3 *continued.*

Site	Bioclimatic zone	Simulation time (years)	PFT* comp.	Individual-based model			Area-based model			Natural vegetation
				NPP	LAI	Biomass	NPP	LAI	Biomass	
Bialowieza, 23°30′E 52°30′N	3	250	NE	0.14	0.9	6.6	0.01	0.1	0.1	Needle-leaved evergreen (*Picea abies*, *Pinus sylvestris*) and broadleaved deciduous forests (mainly dominated by *Quercus* spp., *Carpinus betulus*, *Alnus glutinosa*, *Tilia cordata* and *Acer platanoides*). Seral forest of *Populus tremula* and *Betula* spp. (Falinski, 1986)
			TBS	0.08	0.6	3.1	0.12	0.9	1.4	
			IBS	0.09	0.4	7.9	0.53	3.0	7.0	
			G	0.02	0.6	0.0	0.01	0.0	0.0	
		2000	NE	0.20	1.2	32.6	0.00	0.0	0.2	
			TBS	0.13	0.9	12.2	0.68	4.2	26.6	
			IBS	0.00	0.0	0.0	0.00	0.0	0.0	
			G	0.00	0.0	0.0	0.01	0.0	0.0	
N France, 02°E 48°N	7	250	TBS	0.13	0.9	5.6	0.30	2.1	3.8	Deciduous *Quercus* spp.-dominated forest with *Fraxinus excelsior*, *Ulmus campestris*, *Tilia* spp., *Prunus avium*, *Corylus avellana* and *Carpinus betulus* (Council of Europe, 1987)
			IBS	0.19	0.8	15.7	0.39	2.2	4.2	
			G	0.07	2.2	0.1	0.00	0.0	0.0	
		2000	TBS	0.40	2.8	34.2	0.73	4.2	26.3	
			IBS	0.00	0.0	0.0	0.00	0.0	0.0	
			G	0.02	0.5	0.0	0.01	0.0	0.0	
Derborence, 07°E 46°N	1	250	NE	0.18	1.2	7.8	0.05	0.4	0.6	Montane evergreen needleleaf forest dominated by *Abies alba* and *Picea abies*, with *Pinus* spp. as secondary element, and seral deciduous component (needle-leaved *Larix decidua*; broadleaved *Populus tremula*; *Salix* spp.; *Betula* spp.; *Sorbus aucuparia*) (Kraeuchi, 1994)
			IBS	0.07	0.4	4.7	0.71	4.2	9.5	
			G	0.08	2.6	0.1	0.01	0.0	0.0	
		2000	NE	0.35	2.0	52.4	0.81	4.8	31.6	
			IBS	0.00	0.0	0.0	0.00	0.0	0.0	
			G	0.00	0.1	0.0	0.00	0.0	0.0	
Lombardy, 09°E 45°30′N	6	250	TBS	0.13	0.9	6.0	0.24	1.8	3.0	Broadleaved deciduous forest of *Quercus robur*, *Ulmus campestris*, and *Carpinus betulus* (Council of Europe, 1987)
			IBS	0.15	0.6	13.6	0.45	2.5	5.2	
			G	0.10	3.0	0.1	0.01	0.0	0.0	
		2000	TBS	0.44	3.0	41.7	0.74	4.5	28.0	
			IBS	0.00	0.0	0.0	0.00	0.0	0.0	
			G	0.02	0.5	0.0	0.01	0.0	0.0	

Table 3 *continued.*

Site	Bioclimatic zone	Simulation time (years)	PFT* comp.	Individual-based model			Area-based model			Natural vegetation
				NPP	LAI	Biomass	NPP	LAI	Biomass	
E. Bulgaria, 27°30′E 43°30′N	9	250	TBS	0.05	0.3	1.3	0.25	1.6	3.0	Mixed broadleaved deciduous forest and herbaceous steppe (Walter, 1979)
			IBS	0.11	0.4	7.2	0.28	1.5	2.8	
			G	0.52	15.9	0.5	0.01	0.0	0.0	
		2000	TBS	0.11	0.7	8.0	0.30	1.8	4.9	
			IBS	0.00	0.0	0.0	0.23	1.2	2.6	
			G	0.54	16.7	0.6	0.00	0.0	0.0	
Galicia, 08°W 43°N	8	250	TBS	0.01	0.1	0.3	0.03	0.3	0.4	Mixed deciduous and evergreen broadleaved forest and scrub with *Quercus robur*, *Castanea sativa*, *Pyrus communis* and *Ruscus aculeatus.* Evergreen component includes *Ilex aquifolium*, *Quercus suber*, *Q. ilex*, *Arbutus unedo*, *Phillyrea media* and *Laurus nobilis* (Council of Europe, 1987)
			IBS	0.08	0.3	6.9	0.25	1.5	3.8	
			BE	0.32	2.5	15.4	0.12	1.2	1.7	
			G	0.00	0.0	0.0	0.12	0.3	0.0	
		2000	TBS	0.00	0.0	0.0	0.09	0.6	2.3	
			IBS	0.00	0.0	0.0	0.04	0.2	0.7	
			BE	0.49	3.5	48.0	0.30	2.5	7.8	
			G	0.00	0.0	0.0	0.01	0.0	0.0	
Apulia, 17°E 40°30′N	10	250	IBS	0.13	0.5	14.4	0.33	2.0	4.5	Mixed deciduous and evergreen forests, dominated by deciduous *Quercus pubescens*, *Ostrya carpinifolia* and *Carpinus orientalis* and evergreen *Quercus ilex* and *Pistacia lentiscus* (Council of Europe, 1987; Debazac, 1983)
			BE	0.30	2.3	13.6	0.06	0.6	0.8	
			G	0.00	0.0	0.0	0.09	0.4	0.1	
		2000	IBS	0.00	0.0	0.0	0.28	1.6	3.7	
			BE	0.55	3.8	53.9	0.11	0.9	2.2	
			G	0.00	0.0	0.0	0.07	0.3	0.1	

* NE = needle-leaved evergreen; TBS = shade-tolerant broadleaved summergreen; IBS = shade-intolerant broadleaved summergreen; BE = broadleaved evergreen; G = grass.

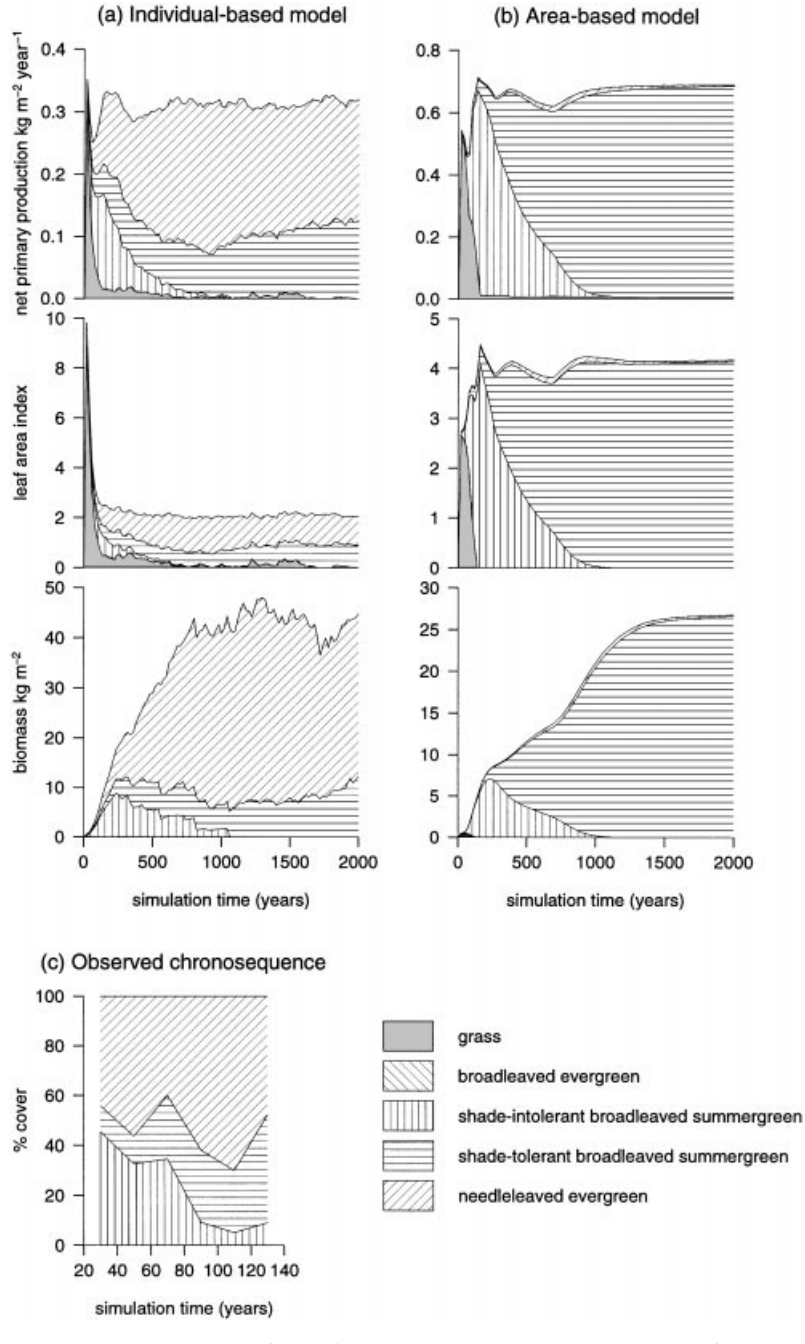

Fig. 3 Net primary production (kgC m^{-2} years^{-1}), leaf area index and biomass (kgC m^{2}) for plant functional types (PFTs) predicted by: (a) the individual-based model; (b) the area-based model for a 2000-years time sequence under a modern climate at site Bialowieza (23°30′E 52°30′N); and (c) a chronosequence of relative cover of woody functional types based on observations in 10 community types in the Bialowieza Forest (after Falinski, 1986).

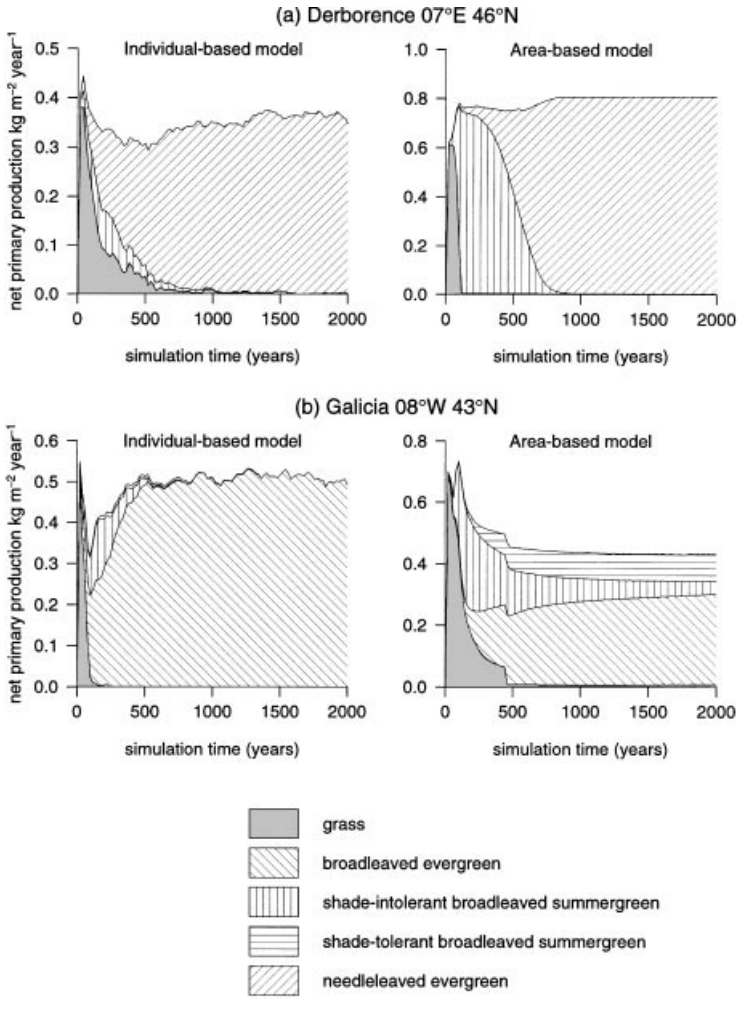

Fig. 4 Net primary production (kgC m^{-2} $year^{-1}$) of plant functional types (PFTs) predicted by (i) the individual-based model, and (ii) the area-based model for a 2000-years time sequence under a modern climate at (a) Derborence (07°E 46°N) and (b) Galicia (08°W 43°N).

low and trees (and grasses) allocate more of their production to roots than to leaves. This results in a low tree LAI, and ample PAR reaches the grass layer.

Quantitatively, both models produce NPP, LAI and biomass predictions that are within the ranges expected for temperate and boreal ecosystems. Equilibrium biomass values generated by the models are generally somewhat higher than observations. However, predictions of community biomass are very sensitive to mortality rates, which determine the average longevity of individuals and, therefore, the time available for the accumulation of biomass as heartwood. Since no disturbance or harvesting regime was applied in the simulations carried out in this study, the average longevity of trees was higher than commonly observed in nature, and considerably higher than in many managed ecosystems, and this would lead to an exaggerated prediction of average biomass for the regional scale.

The area-based model generally produced higher NPP and LAI predictions than the individual-based

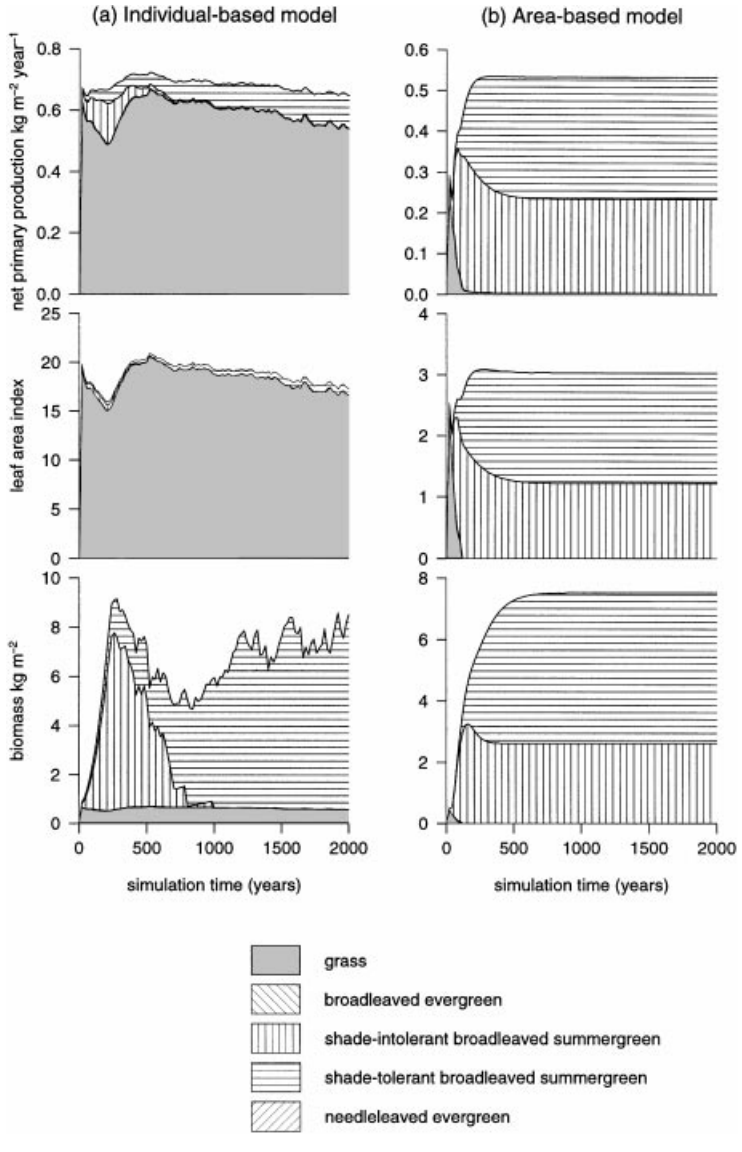

Fig. 5 Net primary production (kgC m^{-2} $year^{-1}$), leaf area index and biomass (kgC m^{-2}) for plant functional types (PFTs) predicted by: (a) the individual-based model, and (b) the area-based model, for a 2000-years time sequence under a modern climate in E Bulgaria (27°30′E 43°30′N).

model. This is at first surprising, since the processes of photosynthesis, respiration and allocation of carbon, which fundamentally control total ecosystem production, are formulated the same way in the two models. The reason for the generally lower NPP values in the individual-based model appears to be the opportunity for 'leakage' of light to the forest floor, which can account for a large fraction (> 50%) of total incident PAR when tree LAI is relatively low, but ground-level conditions are still too shady for growth of the (relatively light-demanding) grass. By contrast, in the area-based model, where there is no explicit vertical structure, exactly 50% of PAR is always

utilized for photosynthesis in that proportion of the modelled area occupied by vegetation.

Competition among plants for the major resources of light, water, nutrients and space is primarily a neighbourhood-scale process (e.g. Aarssen, 1992). Recent developments in ecosystem modelling demonstrate that abstraction of the outcomes of competition to scales much broader than the neighbourhood is possible, and can plausibly reproduce real biogeographic patterns, at least for rather broadly defined PFTs and at the target precision-level of continental and global-scale studies (Cramer *et al.*, 2001; Kucharik *et al.*, 2000; Sitch, 2000). The present study demonstrates that an area-based model can be further configured to simulate correctly the natural succession and potential vegetation under the majority of regional climates represented in a continent (Europe) today. However, the area-based model, in common with any vegetation dynamic model that does not explicitly treat patch–scale interactions among individual plants, is phenomenological in the way it represents vegetation dynamics, and this implies that it may fail when driven by conditions other than those under which it is calibrated and tested (Pacala & Deutschman, 1995). The marginally poorer performance of the area-based model compared with the individual-based model at a number of sites in this study provides a hint of this limitation. The individual-based model is mechanistic in its treatment of competition for light and water (and implicitly, space), and for this reason presumably more robust when applied beyond the limits of the environmental space for which its performance is known.

CONCLUSIONS

In general, the area-based model overestimates the proportional abundance of deciduous woody vegetation in areas where deciduous and evergreen types coincide. It also overestimates the abundance of woody vegetation in comparison to grasses in areas characterized by pronounced seasonal water deficits. In both these types of environment, the individual model produces a closer match to reality. The differences between the predictions of the models can be traced to their treatment of individual-level processes, in particular light competition and stress-induced mortality.

Our results for the European environment suggest that an explicit individual-based approach to vegetation dynamics may be an advantage in modelling of ecosystem structure and function at the resolution required for regional- to continental-scale studies.

ACKNOWLEDGMENTS

We thank Mike Apps and an anonymous referee for their constructive remarks. This work was part-funded by the European Union project ETEMA (Contract No. ENV4-CT95–0052).

SUPPLEMENTARY MATERIAL

The Appendix to this paper is available from http://www.blackwell-science.com/products/journals/suppmat/GEB/GEB256/GEB256sm.htm

REFERENCES

Aarssen, L.W. (1992) Causes and consequences of variation in competitive ability in plant communities. *Journal of Vegetation Science*, **3**, 165–174.

Busing, R.T. (1991) A spatial model of forest dynamics. *Vegetatio*, **92**, 167–179.

Council of Europe (1987) *Map of the natural vegetation of the member countries of the European Community and the Council of Europe*, 2nd edn. Commission of the European Communities, Luxembourg.

Cramer, W., Bondeau, A., Woodward, F.I., Prentice, I.C., Betts, R.A., Brovkin, V., Cox, P.M., Fisher, V., Foley, J.A., Friend, A.D., Kucharik, C., Lomas, M.A., Ramankutty, N., Sitch, S., Smith, B., White, A. & Young-Molling, C. (2001) Global response of terrestrial ecosystem structure and function to CO_2 and climate change: results from six dynamic global vegetation models. *Global Change Biology*, **7**, 357–373.

Czárán, T. & Bartha, S. (1989) The effect of spatial pattern on community dynamics; a comparison of simulated and field data. *Vegetatio*, **83**, 229–239.

Debazac, E.F. (1983) Temperate evergreen forests of the Mediterranean region and Middle East. *Temperate broad-leaved evergreen forests. Ecosystems of the world*, vol. 10 (ed. by J.D. Ovington), pp. 107–123. Elsevier, Amsterdam.

Falinski, J.B. (1986) *Vegetation dynamics in temperate lowland primeval forest: ecological studies in Bialowieza Forest*. Junk, Dordrecht.

Foley, J.A., Prentice, I.C., Ramankutty, N., Levis, S., Pollard, D., Sitch, S. & Haxeltine, A. (1996) An integrated biosphere model of land surface processes, terrestrial carbon balance, and vegetation dynamics. *Global Biogeochemical Cycles*, **10**, 603–628.

Fulton, M.R. (1991) Adult recruitment as a function of juvenile growth in size-structured plant populations. *Oikos*, **61**, 102–105.

Gignoux, J., Menaut, J.C., Noble, I.R. & Davies, I.D. (1998) A spatial model of savanna function and dynamics: model description and preliminary results. *Dynamics of tropical communities*, (ed. by D.M. Newbery, H.H.T. Prins and N.D. Brown), pp. 361–383. Blackwell Scientific Publications, Oxford.

Harper, J.L. (1977) *Population biology of plants*. Academic Press, London.

Haxeltine, A. & Prentice, I.C. (1996) BIOME3: an equilibrium terrestrial biosphere model based on ecophysiological constraints, resource availability, and competition among plant functional types. *Global Biogeochemical Cycles*, **10**, 693–709.

Huang, S., Titus, S.J. & Wiens, D.P. (1992) Comparison of nonlinear height–diameter functions for major Alberta tree species. *Canadian Journal of Forest Research*, **22**, 1297–1304.

Kraeuchi, N. (1994) Modelling forest succession as influenced by a changing environment. *Mitteilungen der Eidgenossischen Forschungsanstalt für Wald, Schnee und Landschaft*, **69**, 143–271.

Kucharik, C.J., Foley, J.A., Delire, C., Fisher, V.A., Coe, M.T., Lenters, J.D., Young-Molling, C., Ramankutty, N., Normal, J.M. & Gower, S.T. (2000) Testing the performance of a Dynamic Global Ecosystem Model: water balance, carbon balance, and vegetation structure. *Global Biogeochemical Cycles*, **14**, 795–825.

Landsberg, J.J. (1986) *Physiological ecology of forest production*. Academic Press, San Diego, California.

Leemans, R. & Prentice, I.C. (1989) *FORSKA, a general forest succession model*, vol. 2. Meddelanden Från Växtbiologiska Institutionen, Uppsala.

Lloyd, J. & Taylor, J.A. (1994) On the temperature dependence of soil respiration. *Functional Ecology*, **8**, 315–323.

Menaut, J.C., Gignoux, J., Prado, C. & Clobert, J. (1990) Tree community dynamics in a humid savanna of the Côte-d'Ivoire: modelling the effects of fire and competition with grass and neighbours. *Journal of Biogeography*, **17**, 471–481.

Monsi, M. & Saeki, T. (1953) Über den lichtfaktor in den Pflanzengesellschaften und seine Bedeutung für die Stoffproduktion. *Japanese Journal of Botany*, **14**, 22–52.

Pacala, S.W., Canham, C.D., Saponara, J., Silander, J.A. Jr, Kobe, R.K. & Ribbens, E. (1996) Forest models defined by field measurements: estimation, error analysis and dynamics. *Ecological Monographs*, **66**, 1–43.

Pacala, S.W., Canham, C.D. & Silander, J.A. Jr (1993) Forest models defined by field measurements: I. The design of a northeastern forest simulator. *Canadian Journal of Forest Research*, **23**, 1980–1998.

Pacala, S.W. & Deutschman, D.H. (1995) Details that matter: the spatial distribution of individual trees maintains forest ecosystem function. *Oikos*, **74**, 357–365.

Påhlsson, L. (1994) *Vegetationstyper I Norden*. Nordiska Ministerrådet, Copenhagen.

Prentice, I.C. & Helmisaari, H. (1991) Silvics of north European trees: compilation, comparisons and implications for forest succession modelling. *Forest Ecology and Management*, **42**, 79–93.

Prentice, I.C. & Leemans, R. (1990) Pattern and process and the dynamics of forest structure: a simulation approach. *Journal of Ecology*, **78**, 340–355.

Prentice, I.C., Sykes, M.T. & Cramer, W. (1993) A simulation model for the transient effects of climate change on forest landscapes. *Ecological Modelling*, **65**, 51–70.

Reich, P.B., Walters, M.B. & Ellsworth, D.S. (1992) Leaf life-span in relation to leaf, plant and stand characteristics among diverse ecosystems. *Ecological Monographs*, **62**, 365–392.

Ryan, M.G. (1991) Effects of climate change on plant respiration. *Ecological Applications*, **1**, 157–167.

Sharpe, P.J.H., Walker, J., Penridge, L.K., Wu, H.I. & Rykiel, E.J. Jr (1986) Spatial considerations in physiological models of tree growth. *Tree Physiology*, **2**, 403–422.

Shinozaki, K., Yoda, K., Hozumi, K. & Kira, T. (1964) A quantitative analysis of plant form — the pipe model theory I. *Japanese Journal of Ecology*, **14**, 97–105.

Shmida, A. & Ellner, S. (1984) Coexistence of plant species with similar niches. *Vegetatio*, **58**, 29–55.

Simioni, G., Le Roux, X., Gignoux, J. & Sinoquet, H. (2000) Treegrass: a 3D, process-based model for simulating plant interactions in tree-grass ecosystems. *Ecological Modelling*, **131**, 47–63.

Sitch, S. (2000) The role of vegetation dynamics in the control of atmospheric CO_2 content. Doctoral Dissertation, Lund University, Lund, Sweden.

Sprugel, D.G., Ryan, M.G., Brooks, J.R., Vogt, K.A. & Martin, T.A. (1995) Respiration from the organ level to the stand. *Resource physiology of conifers*, (ed. by W.K. Smith and T.M. Hinckley), pp. 255–300. Academic Press, San Diego, California.

Sykes, M.T., Prentice, I.C. & Cramer, W. (1996) A bioclimatic model for the potential distributions of north European tree species under present and future climates. *Journal of Biogeography*, **23**, 203–233.

Sykes, M.T., Prentice, I.C., Smith, B., Cramer, W. & Venevsky, S. (2001) An introduction to the European Terrestrial Ecosystem Modelling Activity. *Global Ecology and Biogeography*, **10**, 581–593.

Tutin, T.G., Heywood, V.H., Burges, N.A., Moore, D.M., Valentine, D.H., Walters, S.M. & Webb, D.A., eds. (1964–80) *Flora Europaea*, 5 vols. Cambridge University Press, Cambridge.

Walter, H. (1979) *Vegetation of the earth and ecological systems of the geo-biosphere*, 2nd edn. Springer-Verlag, New York.

Zeide, B. (1993) Primary unit of the tree crown. *Ecology*, **74**, 1598–1602.

Representation of vegetation dynamics in modelling of terrestrial ecosystems: comparing two contrasting approaches within European climate space

Benjamin Smith, Colin Prentice & Martin Sykes

[A] APPENDIX: MODEL FORMULATIONS

This appendix supplements the general description of the individual-based and area-based models, given in the main text. Biogeochemical cycling and its component processes of photosynthesis, evapotranspiration and water exchange within the models closely follows the approach of BIOME3 (Haxeltine & Prentice, 1996). Process equations and other details are given by Haxeltine & Prentice and are not repeated here except where the original approach has been modified.

[B] Insolation and potential evapotranspiration

Net incident photosynthetically active radiation (PAR) and potential evapotranspiration (PET) are calculated for the middle day of each month, based on quasi-daily values (i.e. monthly means linearly interpolated to yield a value for each day) for surface air temperature and fraction of full sunshine (see Haxeltine & Prentice, 1996).

[B] Soil hydrology

Soil hydrology is modelled according to the approach of BIOME3. Availability of water for plant growth is based on storage and flow within a two-layered soil profile. Water enters the upper soil layer (0-0.5 m) through precipitation, or melting of snow from a dynamic snow pack. On days with an average temperature ≤–2°C, precipitation does not enter the soil directly but replenishes the snow pack. Evapotranspiration by vegetation (actual evapotranspiration, AET) depletes the water content of the soil. Uptake by plants is partitioned according to the PFT-specific fraction of roots situated in each layer (see Table 2). Additional depletion of soil water may occur through percolation beyond the lower soil layer (0.5-1.5 m) and out of reach by plant roots, while precipitation onto a saturated upper soil layer is lost as surface runoff.

In the individual-based model, water content in each soil layer, and storage in the snow pack, are modelled independently for each patch, based on the overall precipitation and temperature and patch-specific vegetation dynamics; i.e. there are no horizontal fluxes of water between patches.

In the present study, all soils were assumed to have a volumetric holding capacity (H_{max}) of 11%, and Haxeltine & Prentice's percolation coefficient K was set to 5.0 mm day^{-1}.

[B] Model state variables and plant allometry

In both models individuals are represented by their carbon biomass (in gC) in three living tissue compartments – leaves (C_{leaf}), fine roots (C_{root}) and sapwood ($C_{sapwood}$) – and in heartwood ($C_{heartwood}$). Grasses have leaf and root compartments only; i.e. $C_{sapwood}$ and $C_{heartwood}$ are undefined.

For trees, height (H, m), mean stem diameter (D, m), and crown area (CA, m^2) can be derived from the biomass values by the allometric relations (Huang *et al.* 1992, Zeide 1993):

$$D = \left[\frac{4 \times (C_{\text{sapwood}} + C_{\text{heartwood}})}{WD.\pi.k_{\text{allom}2}} \right]^{1/(2+k_{\text{allom}3})} \quad (1)$$

$$H = k_{\text{allom}2}.D^{k_{\text{allom}3}} \quad (2)$$

$$CA = \min(k_{\text{allom}1}.D^{k_{\text{rp}}}, CA_{\max}) \quad (3)$$

where k_{allom1}, k_{allom2}, k_{allom3} and k_{rp} are constants, WD is wood density (gC m^{-3}) and $CA_{\max}$ is maximum crown area (m^2) (see Table A1).

[B] Upscaling from the individual to the region

In the area-based model, each PFT is represented by a single individual with properties reflecting the current average for the PFT over the area modelled. For trees, scaling of biomass to the regional scale is achieved by multiplying individual values by N, the average density of individuals of the PFT over the area modelled (m^{-2}). The value of N is updated each yearly time-step, based on changes in population density due to establishment and mortality (see below). Fractional PFT areal cover (called foliar projective cover, FPC) is related to mean individual leaf area index by the Lambert-Beer law (Monsi & Saeki, 1953; Prentice *et al.*, 1993), under the assumption that success of a PFT 'population' in competition for space will be proportional to competitive ability for light in the vertical profile of the forest canopy:

$$FPC = CA.N.\left[1 - \exp(-0.5LAI_{\text{ind}})\right] \quad (4)$$

where

$$LAI_{\text{ind}} = C_{\text{leaf}}.SLA / CA \quad (5)$$

where SLA is specific leaf area, the ratio of leaf area to mass (m^2 $[gC]^{-1}$), a PFT-specific constant (see Table 2).

In the individual-based model, regional properties are the taken as the average over the 10 patches, which represent random samples of the regional vegetation. In each patch, all tree individuals of sapling size or above are represented explicitly, whereas grasses are represented as one 'individual' having each of the C3 and C4 photosynthetic pathways, and spanning the entire patch (though potentially with LAI<1) at ground level.

[B] Leaf phenology

Fractional leaf coverage is updated daily for summergreen trees and grasses. Leaf expansion begins when the daily mean temperature (T) reaches 5°C, after which fractional cover increases linearly with accumulated growing-degree days on a 5°C base (GDD_5, i.e. the sum of [T–5], updated daily), achieving full cover at GDD_5 = 200 (trees) or 50 (grasses). Leaves are shed when daily mean temperature falls below 5°C. Grasses can also shed their leaves under conditions of severe water stress, i.e. when available soil moisture levels fall below 35% of water holding capacity.

[B] Photosynthesis and water exchange

Photosynthesis and actual evapotranspiration (AET) are calculated codependently by a coupled carbon and water flux module, as described by Haxeltine & Prentice (1996). The variables driving the model are FPAR, the fraction of incoming radiation intercepted by green vegetation; the atmospheric partial pressure of CO_2 (a constant in the present experiment); and mean daily air temperature. AET is constrained by available soil moisture (see above) and potentially limits photosynthesis via canopy conductance. The key output of the module is gross photosynthesis on a canopy area-basis, A_{gd} (gC m^{-2} day^{-1}) given by:

$$A_{gd} = A_{nd} + R_d \quad (6)$$

where A_{nd} is net photosynthesis, and R_d leaf respiration (both in units of gC m^{-2} day^{-1}). Mid-monthly values of A_{gd} are multiplied by the number of days in the month to give monthly gross primary production (GPP, gC m^{-2}).

[C] *Area-based model*

In the area-based model, photosynthesis calculations are performed for the middle day of each month, with AET calculations performed daily. FPAR is set to FPC for each PFT.

[C] *Individual-based model*

In the individual-based model, photosynthesis and AET calculations are performed daily. For trees, FPAR is set to the fraction of incident light captured by each tree in the patch, calculated by the Lambert-Beer law:

$$I(z) = I(0).\exp\left[-0.4L_*(z)\right] \quad (7)$$

where $I(z)$ is the PAR level at canopy depth z and $L_*(z)$ is the accumulated LAI of all trees in the patch above canopy depth z. PAR uptake by each individual is calculated by integrating Equation (7) for 1 m layers from the top of the canopy to the forest floor (Prentice *et al.*, 1993).

For grasses, FPAR is the proportion of PAR reaching the forest floor (i.e. not taken up by trees), multiplied by grass LAI (i.e. the fractional area covered by grass leaves), if this is less than 1. Grass FPAR is partitioned between C3 and C4 grasses in proportion to their relative LAI.

[B] Autotrophic respiration

A proportion of assimilated carbon is lost as maintenance respiration by living tissue. Respiration rates are calculated daily and follow a modified Arrhenius dependence on temperature (Lloyd & Taylor, 1994; Haxeltine & Prentice, 1996). For a particular tissue, *t*, maintenance respiration is given by:

$$R_{m,t} = 0.0548 \times r.\frac{C_t}{cton_t}.\exp\left[308.56 \times \left(\frac{1}{56.02} - \frac{1}{T - 45.87}\right)\right] \quad (8)$$

where r is a PFT-specific respiration coefficient (see Table 2); C_t is the carbon content of tissue t on a canopy-area basis; $cton_t$ is the (constant) carbon-nitrogen mass ratio of tissue t

(see Table A1; Ryan, 1991; Sprugel *et al.*, 1995); and T is ambient temperature. For the leaf compartment, respiration is scaled linearly to daily leaf cover.

Growth respiration is accounted for by a 25% reduction in the carbon remaining following deduction of maintenance respiration from gross photosynthesis (Ryan, 1991), i.e.

$$R_g = 0.25 \times (GPP - R_m) \quad (9)$$

where R_m is total maintenance respiration, i.e. (R_{leaf} + R_{root} + $R_{sapwood}$). Net primary production (NPP, gC m^{-2}) is then given by:

$$NPP = GPP - R_m - R_g \quad (10)$$

[B] Tissue turnover

A proportion of leaf, root and sapwood tissue is turned over (i.e. lost as living tissue) each year. Leaf and root turnover is assumed to enter the litter, whereas turned-over sapwood is converted to heartwood:

$$C_{t,new} = C_{t,old}.(1 - turn_t) \quad (11)$$

where $turn_t$ is the turnover rate ($year^{-1}$) for tissue t (see Table 2).

[B] Reproduction

A constant proportion (10%) of annual NPP is assumed to be allocated to reproduction, e.g. production of flowers, cones, seeds and vegetative propagules (Harper, 1977):

$$C_{repr} = 0.1 \times NPP \quad (12)$$

[B] Allocation

Assimilated carbon remaining after accounting for respiration and allocation to reproduction is available for allocation to the living tissue compartments as new biomass. Allocation is performed once per annual time step. For trees, an optimisation attempts to satisfy simultaneously the allometric relationships:

$$LA = k_{la:sa}.SA \quad (13)$$
$$C_{leaf} = ltor.wscal.C_{root} \quad (14)$$
$$H = k_{allom2}.D^{k_{allom3}} \quad (15)$$
$$CA = \min(k_{allom1}.D^{k_{rp}}, CA_{max}) \quad (16)$$

where SA is mean sapwood cross-sectional area ($C_{sapwood}/WD/H$, m^2); $k_{la:sa}$ is a constant (see Table A1); $ltor$ is a PFT-specific constant (see Table 2); and $wscal$ is a PFT-specific index of water availability, updated annually, representing the mean fraction of water holding capacity in the upper soil layer, on days with non-zero leaf cover by the PFT (see Haxeltine & Prentice, 1996). Equation (13) implements the Pipe Model, a constant ratio of leaf area to sapwood cross-sectional area (Shinozaki *et al.* 1964); while Equation (14) implements a

functional-balance response to water availability, i.e. increased allocation to roots versus shoots under conditions of water stress. Translocation of carbon between tissues (i.e. negative allocation to one tissue to permit positive allocation to another) is disallowed; a proportion of sapwood is killed if necessary to enable a simultaneous solution.

For grasses, assimilated carbon is allocated among leaves and roots so as to satisfy Equation (14).

[B] Establishment

In both models, bioclimatic limits determine which PFTs are able to establish given the climate at a particular location (see Table 2). For PFTs within their bioclimatic limits, establishment is implemented once per annual time step.

[C] *Area-based model*

In the area-based model, establishment of new individuals is modelled as changes in PFT state variables; i.e. properties of the 'average individual' and individual density. New individuals are introduced as 1.2 m high saplings; i.e. the seedling stage of establishment is not modelled explicitly, but accomodated in the sapling establishment rate.

The overall establishment rate for trees (est_{tree}) is proportional to the fractional ground area not covered by trees. As tree cover approaches 100%, establishment is reduced by the degree of shading under the forest canopy, estimated by the Lambert-Beer law:

$$\begin{aligned} est_{\text{tree}} &= k_{\text{est}}(1 - FPC_{\text{tree}}) && ; FPC_{\text{tree}} \le 0.9 \\ est_{\text{tree}} &= k_{\text{est}} . \left\{1 - \exp\left[-5 \times (1 - FPC_{\text{tree}})\right]\right\}(1 - FPC_{\text{tree}}) && ; FPC_{\text{tree}} > 0.9 \end{aligned} \qquad (17)$$

where FPC_{tree} is the sum of FPC values for all woody PFTs and k_{est} is a constant (see Table A1). Total tree establishment is partitioned among all regenerating woody PFTs according to their maximum establishment rates, current FPCs and the fractional ground area that is sufficiently illuminated, in the month with the highest mean insolation, to allow regeneration. For a particular PFT,

$$est = est_{\text{tree}} . \frac{est_{\max}}{\sum_{pft} est_{\max, pft}} . FPC . (1 - \sum_{pft} FPC_{pft}) \qquad (18)$$

where $est_{\max}$ is a PFT-specific maximum establishment rate (saplings.year^{-1}; see Table 2); the *FPC* summation is over PFT's for which ($PAR_{\max}$.exp[–0.4*LAI*] < $par_{\min}$); $PAR_{\max}$ is the PAR level (Wm^{-2}) of the month having the highest mean insolation; and $par_{\min}$ is the target PFT's minimum PAR level for establishment (Wm^{-2}; see Table 2).

The establishment rate modifies the density of individuals:

$$N_{\text{new}} = N_{\text{old}} + est \qquad (19)$$

and updates each of the four biomass compartments (t):

$$C_{t,\text{new}} = \frac{C_{t,\text{old}} . N_{\text{old}} + C_{t,\text{sapl}} . est}{N_{\text{new}}} \qquad (20)$$

where $C_{t,\mathrm{sapl}}$ is the biomass in compartment *t* for a sapling of height 1.2 m, derivable from the allometry Equations (1-3).

[C] *Individual-based model*

In the individual-based model, tree establishment is modelled directly by introduction of new individuals with the character of saplings. The number of new saplings of a PFT established in a patch in a given year is a number drawn from the Poisson distribution with expectation:

$$\mu(F).est_{\max}.\left(k_{\mathrm{reprod}}.C_{\mathrm{repr}} + k_{\mathrm{bgestab}}\right) \quad (21)$$

where *F* represents potential productivity for the current PFT at the forest floor, as a fraction of the maximum possible; k_{reprod} and k_{bgestab} are constants; and

$$\mu(F) = \exp\left[\alpha(1-1/F)\right] \quad (22)$$

where α is a PFT-specific constant. The function μ, which ranges from 0-1, captures non-linearity in the recruitment rate of adults relative to growing conditions in the understorey (Fulton 1991). The PFT-specific values of α (Table 2) reflect the expected growth rate-recruitment relationship, given the characteristic life history class ('pioneer' versus 'climax') of the PFT.

New individuals are given an initial biomass proportional to current potential NPP at the forest floor; under full illumination this produces saplings approximately 1.2 m in height.

[B] Mortality

[C] *Area-based model*

Mortality is modelled by changes to the average-individual state variables and individual density. For trees, fractional mortality is the sum of a base rate ($mort_{\min}$, the inverse of PFT-specific mean non-stressed longevity, *long*; see Table 2); a component based on shading stress ($mort_{\mathrm{shade}}$), intended to affect mainly shade-intolerant PFTs as forests approach canopy closure; and a component based on growth efficiency, capturing the negative effect of reductions in resource uptake on persistence ($mort_{\mathrm{greffic}}$; c.f. Prentice *et al.*, 1993):

$$mort = mort_{\min} + mort_{\mathrm{greffic}} + mort_{\mathrm{shade}} \quad (23)$$

where

$$mort_{\min} = long^{-1} \quad (24)$$

$$mort_{\mathrm{greffic}} = k_{\mathrm{mort1}}{}^{-1}.\left(1 + k_{\mathrm{mort2}}.\frac{NPP}{C_{\mathrm{leaf}}.SLA}\right) \quad (25)$$

$$mort_{\mathrm{shade}} = mort_{\max}.\frac{par_{\min}}{k_{\mathrm{par}}}.\exp\left[-5\times(1-FPC_{\mathrm{tree}})\right] \quad (26)$$

where k_{mort1}, k_{mort2} and k_{par} are constants (see Table A1). The mortality rate modifies the density of individuals:

$$N_{new} = N_{old}(1 - mort) \quad (27)$$

and updates each of the four biomass compartments:

$$C_{t,new} = C_{t,old}(1 - mort) \quad (28)$$

[C] *Individual-based model*

Mortality is implemented as a stochastic process in the individual-based model. The probability of an individual being killed each year is the sum of a background rate, the inverse of non-stressed longevity for the PFT to which it belongs, and a much higher rate (0.3), imposed when five-year average growth efficiency falls below a PFT-specific threshold, $greff_{min}$ (Wm^{-2}; see Table 2):

$$mort = \min(mort_{min} + mort_{greff}, 1) \quad (29)$$

where

$$mort_{min} = long^{-1} \quad (30)$$

and $mort_{greff} = 0.3$ if $greff < greff_{min}$; 0 otherwise; where

$$greff = \frac{NPP_5}{C_{leaf}.SLA} \quad (31)$$

and NPP_5 is annual NPP for the individual, averaged over the last five simulation years.

TABLES

Table A1. Values of constants used in the models.

Symbol	Value	Units	Meaning
WD	2×10^5	gC m^{-3}	sapwood and heartwood C density
CA_{max}	27.3	m^2	maximum individual crown area
k_{allom1}	100	-	constant in allometry equations
k_{allom2}	40	-	constant in allometry equations
k_{allom3}	0.85	-	constant in allometry equations
k_{rp}	1.6	-	constant in allometry equations
$cton_{leaf}$	29	-	C:N mass ratio in leaves
$cton_{root}$	330	-	C:N mass ratio in fine roots
$cton_{sapwood}$	29	-	C:N mass ratio in sapwood
$k_{LA:SA}$	8×10^3	-	tree leaf to sapwood area ratio
k_{est}	0.06	-	constant in establishment equations
k_{reprod}	10^{-10}	-	constant in establishment equation
$k_{bgestab}$	10^{-3}	-	constant in establishment equation
k_{mort1}	0.01	-	constant in mortality equations
k_{mort2}	11.9	$(gC)^{-1}$ m^2	constant in mortality equation
k_{par}	4.05	Wm^{-2}	constant in mortality equation